Experimental analysis of vapour bubble growing on a heated surface

T. A. KOWALEWSKI[a*]
J. PAKLEZA[b]
R. TRZCIŃSKI[a]
A. ZACHARA[a]

[a] *Institute of Fundamental Technological Research Polish Academy of Sciences, Świętokrzyska 21*

[b] *LIMSI−CNRS, BP 133, 91403 Orsay Cedex, France*

Abstract   Using high speed video camera and numerical processing of the digital images transient description of the geometry and the interface velocity for vapour bubble growing at the heated surface in subcooled liquid is achieved. Particle Image Velocimetry and Thermometry are applied to obtain details about velocity and temperature in the surrounding flow field. Experimental results are compared with the results of calculations based on a simple mathematical model.

Keywords: Vapour bubble; Evaporation; High speed imaging, PIV & T

Nomenclature

$a = k/\rho c$	–	thermal diffusivity, m^2/s
c	–	specific heat, J/(kg K)
$C = D_b/D$	–	bubble shape parameter
C_1	–	empirical microlayer parameter
D_b	–	base diameter, mm
D_e	–	equivalent diameter, mm
H	–	height of the bubble centre, mm
h_{lv}	–	latent heat of vaporisation, J/kg
Ja $= \rho_l c_l \Delta T/\rho_v h_{lv}$	–	Jakob number

*Corresponding author. E-mail address: tkowale@ippt.gov.pl

k	–	thermal conductivity, W/(m K)
P	–	pressure, kPa
$\mathrm{Pr} = \mu c/k$	–	Prandtl number
T	–	temperature, ^{o}C, K
t	–	time, ms

Greek symbols

δ	–	interface thermal layer thickness, m
μ	–	dynamic viscosity, Ns/m^2
ν	–	kinematic viscosity, m^2/s
ρ	–	density, kg/m^3

Subscripts

l	–	liquid phase
ν	–	vapour phase
s	–	solid phase
sat	–	saturation

1   Introduction

From the recent numerical simulations it is possible to generate solutions describing bubble growth from inception to departure without any assumption being made about the bubble shape but axial symmetry and more or less realistic modelling of the wall contact line. To validate these simulations suitable experimental data are required. The bubble shape and its evolution usually employed for comparison with the simulation results are still useful but need to be completed by measurements of additional quantities. In the following we describe summary of experimental investigations of vapour bubble growth performed in our two laboratories. An image analysis is performed and yields an accurate determination of several relevant parameters. Specific attention is devoted to describe dynamics of the moving bubble interface. Deformation of the interface and frequently observed shape oscillations are analysed to estimate the interface temperature. Velocity and temperature fields in the liquid phase are also visualised seeding the fluid with thermochromic liquid crystals. The simple mathematical model presented in the Appendix has been used to calculate the history of the bubble geometrical parameters in the first stage of its growth.

2　Experimental apparatus and procedure

Isolated bubbles are generated on a horizontal surface inside a 30 cm^3 cube shaped chamber. The working fluid is water boiling under sub-atmospheric pressure. Some experiments are performed for methyl alcohol and PP1 under normal atmospheric pressure. Five walls of the cube are equipped with optical openings for observation or illumination of the internal chamber. In the present experiments the bottom opening is used to mount an electrical heater of a brass plate used for bubbles generation. By changing the metal part of the heater, diameter of the boiling area can be varied in the range from 1 to 20 mm. The cell construction allows for experimentation in the low-pressure environment. The system pressure was controlled in the range 1-100 kPa using a vacuum pump and a 0.5 m^3 reservoir [1].

Back light illumination is applied to obtain images of a well-defined bubble interface. For this purpose both a strobe light or a halogen spot lamp are used. The field of view is approximately 3 mm×3 mm. Several acquisition methods are used to collect images. The high resolution 8-bit images of 768×544 pixels are acquired by standard 50 Hz camera and frame-grabber. Stroboscopic illumination used at steady thermodynamic conditions in the cavity allows us to obtain sequences of high resolution images of bubbles appearing on the heater with a constant period. To verify temporal resolution of the stroboscopic method and to obtain precise description of the selected time regime the multi-exposure procedure is used, with typical 4 – 6 single images overlapping on each frame. Such images after appropriate image filtration and analysis procedure are merged to describe temporal development of the interface. A precise description of the bubble growth process is achieved using a Fastcam-HS40 high speed video camera running from 4500　(full frame) up to 22 500 frames/s. Using this camera up to 8000 images of 256 × 256 pixels are acquired for each run. These images give valuable information on the dynamics of bubble growth and departure, however less accurate in the near wall regions due to the limited spatial resolution of the camera.

A typical image of the bubble observed in the bright field of the parallel light shows dark shadow of the central cross-section with an additional bright spot at the centre. To describe properly the bubble shape the edge extracting technique is applied. The extracted points are used to find a smooth functional representation of the pixel set for the further analysis. This description is used to define the bubble shape, contact angles and,

assuming axial symmetry of the bubble, to calculate its volume. After departure vapour bubbles usually exhibit ellipsoidal shape, which can be well approximated by series of Legendre polynomials. Their coefficients describe degree of deformation for each oscillation mode. The main oblate-prolate deformation of the sphere is given by the amplitude $a_2(t)$ of the fundamental oscillation mode. This method of shape description, already successfully applied to oscillating liquid droplets [2], allows for direct comparison of the shape dynamics with analytical models for free oscillating bubbles. Analysis of these oscillations can deliver information about variation of the surface tension and indirectly indicate variation of the interface temperature.

The flow visualization around the bubble is performed seeding the fluid with thermochromic liquid crystals. Illumination is realized with a 1 mm thick light sheet: a halogen light source is located perpendicularly to the optical axis of the 3 CCD colour camera. The 24-bit images of 576×574 pixels correspond to a field of view of 7.1 mm × 7.1 mm. These images are used for the temperature and velocity evaluation (Particle Image Thermometry and Velocimetry [1]).

3   Selected results

Figure 1 shows typical history of the single vapour bubble observed at low pressure conditions using high speed video imaging. The bubble generation starts at the nucleation site of the wall in the superheated layer of liquid. The measured superheat of the wall necessary to obtain vapour bubbles is about 15 K. Due to the back light illumination, cross section of the bubble appears as a dark shadow. The first observable bubbles have diameter of about 30 μm, far above the inertia controlled growth range, described by the simplified Rayleigh model. The initial growth time is much shorter than the temporal resolution of our system, and measured growth time is close to the total growth time. The bubble presented in Fig. 1 displays a hemispherical shape then turns very rapidly (≈ 0.7 ms) to a truncated spheroid. Afterwards, the bubble grows regularly without any significant modification of its form. At time of about 6 ms, the bubble base shrinks that finally leads to the departure process. The whole bubble growth, from inception to lift-off from the wall takes about 10 ms. Temperature of fluid above the wall boundary layer is about 4 K below saturation temperature. Intensified by the bubble motion cooling of the

interface initiates rapid vapour condensation and finally bubble collapses almost completely. The remaining small residual vapour bubbles have diameter of about 15 μm, close to the system spatial resolution. But before the final bubble implosion takes place a few volumetric oscillations can be observed.
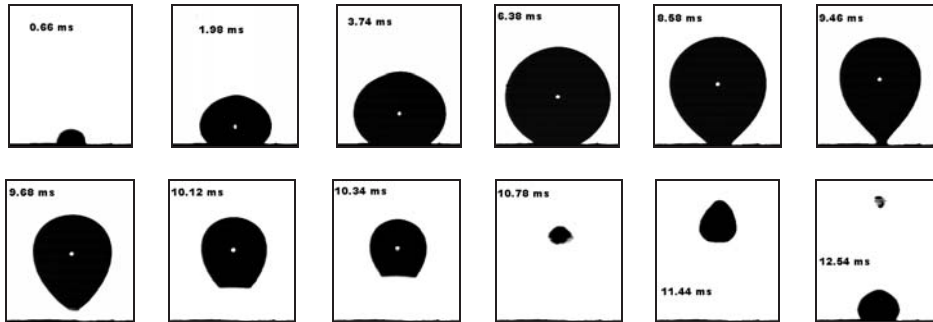

Figure 1. Growth process of a vapour bubble (water $P = 4$ kPa, $T_l = 24.4^\circ$C, $T_s = 46.5^\circ$C) observed at 4500 frames/s by high speed camera. Frames shown at few selected time steps. Bubbles are generated at the hot spot of 1.42 mm diameter. The frame width corresponds to 2.9 mm.
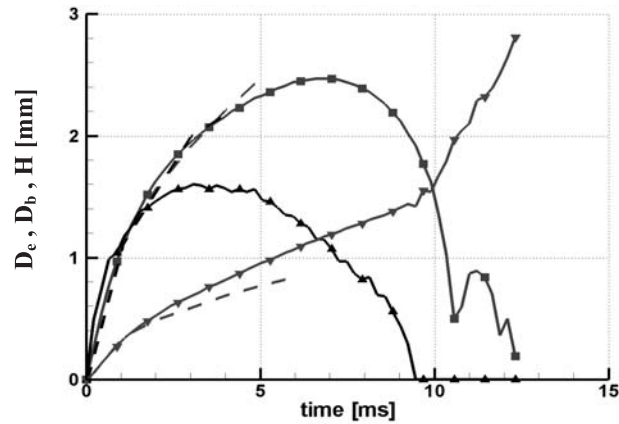

Figure 2. Time history of the bubble equivalent diameter D_e, base diameter D_b and height H of the bubble centre of mass. Experimental results (solid lines) are evaluated from the sequence of 86 images shown in Fig.1, D_e (■), D_b (▲), H (▼). Theoretical results (dashed lines) are calculated from Eqs. (8) and (10), (11), (12).

Figure 2 collects main characteristics of this experiment depicted form the sequence of images. The bubble volume is computed assuming an axial symmetry and D_e, diameter of the equivalent sphere, is plotted together with the bubble base diameter D_b and distance H from the bottom to the bubble centre of mass. The experimental results are compared with theoretical prediction obtained on the base of a simple mathematical model presented in the Appendix. The growth of the bubble may be divided into three main stages. The first one, where all quantities D_e, D_b and H increase with time, corresponds to the early period ($0 < t \leq 2.5$ ms) where strong vaporization is observed, associated with a truncated spheroid growth. In this stage we observe the best agreement between experimental and theoretical results. In a second stage D_b gets smaller while D_e still increases (2.5 ms $\leq t \leq 7.2$ ms). In a third stage the bubble base starts to shrink; the vapour production is not strong enough to balance the deficit at the bubble base, and the bubble diameter D_e decreases. One may see that only during the first 6 ms evaporation exceeds condensation and the net volume of the bubble grows. During this time history the bubble diameter D_e follows very closely $t^{1/2}$ diffusion controlled regime, see Eqs. (8) and (10) in the Appendix. This variation of the diameter as well as that of the base diameter looks qualitatively very similar to numerical prediction of Fujita and Bai [3].
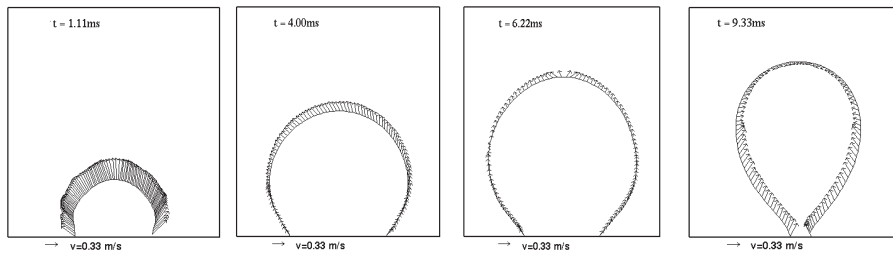

Figure 3. PIV evaluated velocity at the bubble edge. Computations are performed considering two consecutive frames taken at the time interval 0.22 ms.

The PIV method based on Optical Flow approach [4] is used to evaluate local displacements of the contour from tracer-less images of growing vapour bubbles: for each image, the set of pixels corresponding to the bubble contour is first identified. Then, considering two consecutive images separated by a time step of 0.22 ms, the velocity is computed at any point (pixel) of the bubble edge. These calculation results are displayed in Fig. 3

for images from the above described experiment. Initially the growth rate of the bubble is nearly uniform, bubble expands radially outwards displaying this way a hemispherical shape. The highest displacement speed of 1.5 m/s is observed at earliest stages of the bubble growth. After about 6 ms growth rate significantly decreases and becomes restricted mostly to the upper part of the bubble surface. The lower part of the edge, corresponding to the bottom one third of the bubble height, is no longer exposed to vaporization and looks motionless. After about 8 ms the buoyancy starts to elongate the bubble and its lower part is pushed back by the liquid. The bubble no longer expands. The last picture ($t = 9.33$ ms) shows the bubble just before departure, the contact area being nearly zero. The surface speed is negative everywhere and its magnitude is not uniform: the bubble cap looks nearly motionless while the bottom edge contracts by surface tension at increasing velocity (≈ -0.3 m/s). Similar behaviour of the interface can be found in the numerical simulations by Fujita and Bai [3].
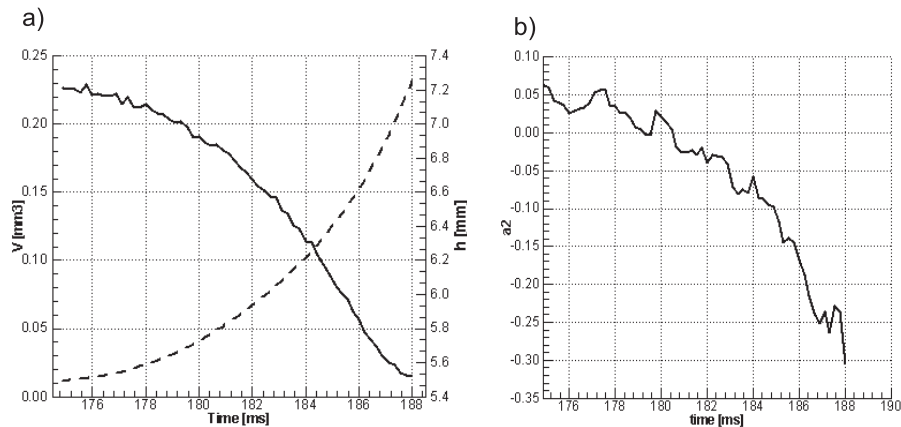

Figure 4. Methyl alcohol vapour bubble departing from the heated surface under atmospheric pressure: a) volume (solid line) and vertical position of the bubble (dashed line); b) deformation parameter a_2.

Observations of vapour bubbles, departing from the surface and quickly collapsing in the upper colder fluid layers, indicate that during this period very often the rising velocity rapidly increases. Sudden change of the added mass obviously accelerates imploding bubble. Figure 4a exemplifies this effect, with strongly decreasing volume, the bubble velocity almost triples before its final size is stabilized. Strong shape oscillations of bubbles departing from the surface are often observed, particularly for alcohol and

PP1 boiling under normal atmospheric pressure. Figure 4b shows temporal variation of the deformation parameter a_2, representing second mode of the Legendre representation for the bubble shape. We may find that initially elongated shape (positive values of a_2), changes to flattened shape as the bubble accelerates. Several characteristic local maxims of the deformation describe observed shape oscillations. The frequency of these oscillations is directly related to the known bubble dimension and to the surface tension. The last parameter strongly varies with temperature and by proper analysis of the phenomenon it can be used as an indicator of the surface supercooling.

The velocity and temperature fields in the liquid phase were investigated applying PIV&T technique. The velocity fields are computed considering the motion of liquid crystal particles and variation of their colour (hue) is analysed to obtain temperature field. An example of such evaluation is given in Fig. 5. The main feature revealed by the tracers is a presence of the convection pattern in the chamber induced by temperature gradients and motion of bubbles.
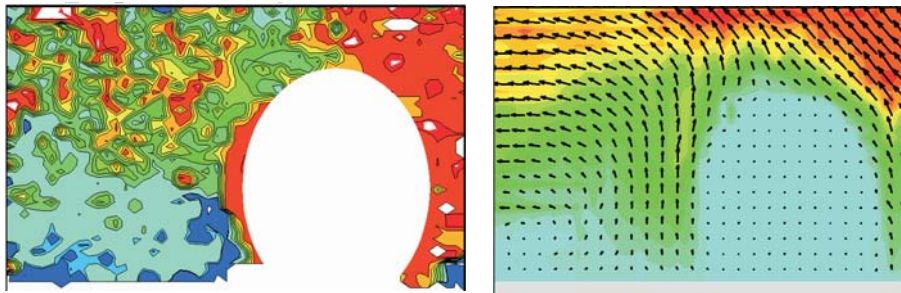

Figure 5. Vapour bubble of water growing at the heated surface: $P = 5.3$ kPa, $T_l = 35.5°$C, $T_s = 66.5°$C. Evaluated temperature field (left) varies from 35°C to 37.5°C, PIV evaluated velocity (right) has maximum magnitude 3 mm/s.

4   Conclusions

Experimental images obtained with a high speed video camera allowed for precise description the bubble growth process from inception to departure. The image analysis made possible a determination of several geometrical parameters in this process such as equivalent diameter, base diameter, height of mass centre and their evolution in time.

Strong shape oscillations of bubbles observed at their departure from the surface are related to the surface tension. Proper analysis of this effect can be used to investigate the surface supercooling owing to strong dependence of surface tension on temperature.

The velocity and temperature fields in the surrounding liquid measured with a thermochromic liquid crystals revealed the occurrence of convection pattern in the chamber and showed complexity of flow effects in the boiling process.

The simple mathematical model presented in Appendix which allows to obtain analytical solution has very limited range of validity. There is a need for precise numerical simulation of fluid flow with a phase change process. The experimental research such as presented in this paper makes possible to achieve this aim.

Received 1 July 2004

References

[1] KOWALEWSKI T. A., PAKLEZA J., CHALFEN J.-B., DULUC M.- C., CYBULSKI A.: *Visualization of vapour bubble growth*, 9th Int. Symposium on *Flow Visualization*, CD-ROM Proceedings, Edinburgh 2000, 176.1-9.

[2] BECKER E., HILLER W.J., KOWALEWSKI T. A.: *Experimental and theoretical investigations of large amplitude oscillations of liquid droplets*, J. Fluid Mech., 231(1991), 189-210.

[3] FUJITA Y. AND BAI Q.: *Numerical simulation of the growth for an isolated bubble in nucleate boiling*, Proc. 11th Int. Heat Transf. Conf., 2(1998), 437-442.

[4] QUNOT G., PAKLEZA J., KOWALEWSKI T. A.: *Particle image velocimetry with optical flow*, Exp. in Fluids, 25(1998), 177-189.

[5] CHEN W. C., KLAUSNER J. F., MEI R.: *A simplified model for predicting vapor bubble growth rates in heterogeneous boiling*, J. Heat Transfer, Trans ASME, 117 (1995), 976-980.

[6] MEI R., CHEN W. C., KLAUSNER J. F.: *Vapor bubble growth in heterogeneous boiling, I – Formulation*, Int. J. Heat Mass Transfer, 38(1995), 909-919.

[7] GENTILE D., PAKLEZA J.: *A numerical simulation of the boiling crisis phenomenon*, (private communication).

[8] HAN C. Y., GRIFFITH P.: *The mechanism of heat transfer in nucleate pool boiling – Part I*, Int. J. Heat Mass Transfer, 8(1965), 887-904.

[9] BANERJEE D., DHIR V. K.: *Study of subcooled film boiling on a horizontal disc, Part I – Analysis*, J.Heat Transfer, Trans. ASME, 123(2001), 271-284.

Appendix

A simple model of the bubble growth, based on the work of previous authors Chen et al. [5], Mei et al. [6], Gentile and Pakleza [7], Han and Griffith [8], Banerjee and Dhir [9], is presented. The bubble is heated by the horizontal solid wall through a super-heated wedge-shaped microlayer of liquid, which evaporates and causes the growth of the bubble. The vapour bubble is surrounded by subcooled liquid, which inhibits the bubble growth and leads to condensation. This process may be described by the energy balance at the liquid-vapour interface

$$\rho_v h_{lv} \frac{dV}{dt} = Q_s - Q_l \,, \tag{1}$$

where V is the bubble volume, Q_s, Q_l are heat flux from the superheated solid wall and heat flux exchanged on the liquid-vapour interface, respectively.

We assume that the bubble has a form of a truncated sphere whose volume V and surface S are expressed as

$$V = \frac{\pi}{6} D^3 \cdot f_1\,(C)\,, \quad f_1\,(C) = 1/2 \cdot \left[1 + 1/2 \cdot \sqrt{1 - C^2} \cdot (2 + C^2)\right] \,, \tag{2}$$

$$S = \pi D^2 \cdot f_2\,(C)\,, \qquad f_2\,(C) = 1/2 \cdot \left[1 + \sqrt{1 - C^2}\right] \,. \tag{3}$$

For $C \rightarrow 1$ the bubble shape approaches a hemisphere and for $C \rightarrow 0$, a sphere.

The heat flux from the superheated wall, calculated following [6], is

$$Q_s = \frac{\pi}{2} \cdot \frac{C^2}{C_1} D^2 \frac{a_l^{1/2}}{\mathrm{Pr}^{1/2}} \rho_l c_l \Delta T_s \cdot t^{-1/2}, \quad \Delta T_s = T_s - T_{sat} \,. \tag{4}$$

The heat flux density at the interface vapour-subcooled liquid is

$$q_l = k_l \cdot \left. \frac{\partial T_l}{\partial r} \right|_{r=R} \cong k_l \cdot \frac{\Delta T_l}{\delta}, \quad \Delta T_l = T_{sat} - T_l \,. \tag{5}$$

where r is a spherical coordinate and R is the radius of the bubble. Then the heat transfer through the interface has the form

$$Q_l = k_l \cdot \frac{\Delta T_l}{\delta} \cdot S \cong k_l \cdot \frac{\Delta T_l}{\delta} \cdot \pi D^2 \cdot f_2(c) \,. \tag{6}$$

For the interface thermal layer thickness δ we take the expression which is used in the solution the thermal conductivity equation (see [8])

$$\delta = (\pi a_l t)^{1/2} \ . \tag{7}$$

Substituting relations (4), (6) and (7) to Eq. (1) we obtain after some transformations the differential equation for the bubble diameter $D(t)$. Its solution has the form (8) obtained at the assumption $C = $ const, where Ja_s and Ja_l are Jacob numbers corresponding to heat transfer from superheated wall and heat transfer to subcooled liquid, respectively [9].

$$D = \frac{2}{f_1(C)} \left[\frac{C^2}{C_1} \cdot \frac{\mathrm{Ja}_s}{(\mathrm{Pr}_l)^{1/2}} - \frac{2}{\sqrt{\pi}} f_2(C) \cdot \mathrm{Ja}_l \right] \cdot (a_l t)^{1/2} \ . \tag{8}$$

Parameter C_1 that appears in relation (4) is determined by the empirical correlation [5]

$$C_1 = 0.00643 \cdot \mathrm{Ja}_s^{0.763} \cdot \mathrm{Pr}_l^{-0.39} \cdot \kappa^{0.0746} \cdot a^{-0.221} \ , \tag{9}$$

where $\kappa = k_l/k_s$, $a = a_l/a_s$.

Now we define the equivalent diameter of the bubble D_e as the diameter of a sphere, which has the same volume as the bubble (2). Hence

$$D_e = [f_1(C)]^{1/3} D \ . \tag{10}$$

The base diameter D_b and the height of the bubble mass centre H are

$$D_b = CD \ , \tag{11}$$

$$H = 1/2 \cdot [\sqrt{1 - C^2} + 3/16 \cdot c^4/f_1(C)] \cdot D \ . \tag{12}$$

Now we shall apply relations (8-12) to our experimental conditions, which are as follows: pressure $P = 4$ kPa, temperatures $T_s = 46.5^{\circ}$C, $T_l = 24,4^{\circ}$C, $T_{sat} = 28,9^{\circ}$C. Hence the wall superheat (4) is $\Delta T_s = 17.6$ K and liquid subcooling (5) $\Delta T_l = 4.5$ K. In this conditions physical parameters of vapour and liquid are: $\rho_v = 0.02856$ kg/m^3, $h_{lv} = 2432.8 \cdot 10^3$ J/kg, $\rho_l = 10^3$ kg/m^3, $c_l = 4.2 \cdot 10^3$ J/kgK $\mu_l = 7.97 \cdot 10^{-4}$ N s/m^2, $k_l = 0.617$ W/mK. On such base we can receive: $a_l = 1.47 \cdot 10^{-7}$ m^{2}s, $\mathrm{Pr}_l = 5.425$, $\mathrm{Ja}_s = 1064$, $\mathrm{Ja}_l = 272$.

To calculate the microlayer parameter C_1 (9), material data of the solid heater are needed. We take the solid wall density $\rho_s = 7.85 \cdot 10^3$ kg/m^3, specific heat $c_s = 0.461 \cdot 10^3$ J/kgK, thermal conductivity $k_s = 100$ W/mK,

hence the thermal diffusivity of the wall is $a_s = 2.7625 \cdot 10^{-5}$ m^2/s. Now we can calculate the lacking parameters in (9) which are $\kappa = 6.17 \cdot 10^{-3}$, $a = 5.3215 \cdot 10^{-3}$ hence we have C$_1$ = 1.476.

The relation $D(t)$ (8) has been obtained assuming that the shape parameter C is constant. In fact this parameter decreases with time t but to illustrate approximately the history of the bubble diameters $D_e(t)$, $D_b(t)$ and the height $H(t)$ it is enough to choose the mean value of parameter C. On the base of the experimental results, for the first stage of the bubble growth, we estimate it as $C = 0.91$.

Making use of the obtained above parameters we have calculated the relation $D(t)$(8) and then $D_e(t)$ (10), $D_b(t)$ (11), $H(t)$ (12). In Fig. 2 these results are compared with the experimental data.

In the first stage of the bubble growth $0 < t < 2.5$ ms (see Fig. 2) the agreement between the experimental and theoretical results is satisfactory. Here the bubble shape does not differ too much from the hemisphere so equivalent and base bubble diameters are nearly equal. It is in agreement with the theoretical model which for $C = 0.91$ gives $D_b/D_e = 0.983$, according to Eqs. (10) and (11). In further stages these results become divergent since simplifying assumptions of this theoretical model are here not valid. Other physical effects must be taken into account that would allow to analyse further history of bubble growth until its detachment. These problems are very complex and need another mathematical formulation. The solution may be obtained by the numerical simulation as it was declared in the Introduction.